



**Controlled synthesis and pH-sensitive complexation of
poly(methacrylic acid) polyampholytes**

Journal:	<i>Polymer Chemistry</i>
Manuscript ID	PY-ART-07-2024-000773.R1
Article Type:	Paper
Date Submitted by the Author:	19-Sep-2024
Complete List of Authors:	Nikishau, Pavel; University of Alabama at Birmingham, Chemistry Kozlovskaya, Veronika; University of Alabama at Birmingham, Department of Chemistry Kharlampieva, Eugenia; The University of Alabama at Birmingham, Chemistry

Controlled synthesis and pH-sensitive complexation of poly(methacrylic acid) polyampholytes

Pavel A. Nikishau,¹ Veronika Kozlovskaya,¹ Eugenia Kharlampieva^{1, &}*

¹Department of Chemistry, &Center for Nanoscale Materials and Biointegration, University of Alabama at Birmingham, Birmingham, AL 35294, USA

*Correspondence to be addressed: ekharlam@uab.edu

Keywords: poly(methacrylic acid), RAFT copolymerization, polymer complexes, coacervates, molecular weight, turbidity.

ABSTRACT: Studies of intra- and intermolecular interactions in pH-responsive polyampholyte solutions are essential for understanding protein molecule solution behavior and cell organelle organization. Understanding and controlling the formation of intra/intermolecular complexes of synthetic polyampholytes can broaden their applications in industry and the biomedical field. Studies of poly(cation-*co*-anion) statistical copolymer solutions with a predominant content of the same-charge groups in the polymer chain are present in the theory when the factual experimental data are underrepresented. Herein, we explored the controlled synthesis of poly(methacrylic acid) copolymers containing primary amine groups and studied the copolymer solution aggregation under various pH and salt conditions. Well-defined poly(methacrylic acid-*co*-3-(aminopropyl)-methacryl amide) copolymers (M_w of 45 kDa and 80 kDa, $\bar{D} < 1.36$) with a varied content of the amine group (PMAA-NH₂ from 2 to 6 mol.%) were synthesized via subsequent reversible addition-fragmentation chain transfer (RAFT) copolymerization. Both computational and experimental studies proved the copolymerization of *tert*-butyl methacrylate with N-(*tert*-

butoxycarbonyl-aminopropyl)methacrylamide where the second monomer is less active in copolymerization due to strong interaction with a chain-transfer agent (CTA). We found that the resulting PMAA-NH₂ copolymers with more than 4 mol.% of amine groups form polyampholyte complexes (PACs) in solution in the pH range from 3.1 to 4.8 due to charge compensation. Given the ability of this PMAA-NH₂ to undergo multilayer assembly at surfaces and controlled crosslinking, our findings can be further expanded to develop advanced and tunable PMAA thin multilayer hydrogels. The synthesis of PMAA-NH₂ copolymers via controlled copolymerization can also lead to facile alternatives for PAC synthesis without using cell-toxic cationic polyelectrolytes such as polyvinylpyridines or polyamines. The copolymers can help develop synthetic routes to novel copolymers and new hydrogel materials with controlled nanostructured architectures, environmentally adaptable microcontinents, PAC-based saloplastics, absorbents, anisotropically structured nanocoatings, and biomedical coatings.

INTRODUCTION

Studies of intra- and intermolecular interactions in pH-responsive polyampholyte solutions are essential for the fundamental understanding of protein molecule solution behavior and cell organelle organization. Understanding and controlling the formation of intra/intermolecular complexes by synthetic polyampholytes can broaden their applications in industry and the biomedical field.^{1,2,3} With their sophisticated structure, biomacromolecules provide a clear example of these forces and their effects on properties.^{1,4,5} Another example is polyelectrolytes, which can create an amorphous blend known as a polymer intermolecular complex, or coacervate, when a mixture of polycation and polyanion is combined.^{6,7,8} This formation occurs because of the strong intermolecular interaction between ionized oppositely charged groups. The recently reignited interest in these polymer complexes and their formation theory has been motivated by

natural polyelectrolytes (*i.e.*, RNA, proteins), which can undergo specific intracellular organization and complex organelle formation.⁹⁻¹²

Poly(methacrylic acid) (PMAA) is a weak polyacid able to form ionic pairs through interacting with polycations,¹³⁻¹⁶ including poly(vinylpyridines),¹⁷ poly(diallyl dimethylammonium) chloride,¹⁸ and other quaternized polyamines.^{19,20} However, such PMAA intermolecular complexes exist only in a narrow composition range when the mole fraction of positively or negatively charged units is close to 0.5 (the equimolar charge ratio). While with the primary amine polycations such as poly(allylamine), PMAA forms insoluble complexes in a broader range of polycation-to-polyanion ratios, even when an excess of one of the polyelectrolyte units is large.^{8,21}

These strongly interacting weak polyelectrolytes form interpolymer complexes in the pH range when the net charge from the ionization of one group is compensated by the ionization of a second, oppositely charged group.^{22,23} In the case of PMAA-based intermolecular complexes, the degree of ionization of carboxyl groups is affected by its pK_a value, which ranges from 5.5-6.0, but the effective pK_a of acidic groups decreases in the presence of amine groups.^{13,22,24,25} Salt concentration also plays a vital role in polyelectrolyte interactions due to the charge screening and can completely dissociate ionically paired interpolymer complexes even under pH conditions favorable for the complex formation.^{26,27,28} For example, Schlenoff's group found that the polyelectrolyte coacervation due to ionic pairing can be regulated by polymer hydrophobicity, where the critical salt concentration at which polyelectrolyte complexes fully dissociates decreases with higher levels of hydrophobic group content.^{17,29}

Polymers bearing cationic and anionic groups on the same chain, termed polyzwitterions, can also form polyzwitterionic complexes at pH ranges when charge compensation is present.³⁰⁻³⁴ Polyzwitterions can have oppositely charged groups on the same monomer unit (known as

polybetaines) or different monomer units (known as polyampholytes) and can self-organize into polyampholyte complexes (PACs).³³⁻³⁶ Alternating polyampholytes like poly(cation-*alt*-anion)^{37,38,39} have the equivalent contents of oppositely charged ionic groups and are the most extensively studied types of polyampholytes. Polyzwitterions undergo intra- and intermolecular complexation at low temperatures, and with enough thermal energy, they break into individual molecules in solution, displaying an upper critical solution temperature in aqueous media.^{34,35,36}

Generally, polyzwitterion and poly(cation-*alt*-anion) PACs exhibit similar solution behavior. For polycation/polyanion polyelectrolyte intermolecular complexes, the concentration of strong electrolytes (*e.g.*, NaCl) and solution pH play a crucial role in the stability of a PAC, affecting ion charge screening and the degree of ionization, respectively. Well-organized alternating copolymers with periodic structures show a unique self-assembly behavior in solution, resulting in the spontaneous formation of micelles or unilamellar vesicles in water in a wide pH range (from 3 to 8).^{40,41}

In contrast, the behavior of random poly(cation-*co*-anion) polyampholyte copolymer solutions is less extensively studied.³¹ They can be easily synthesized by copolymerization of monomers potentially carrying positive or negative charges, while the ratio of monomers and their reactivity can control the polyampholyte net charge.^{38,42,43} However, the final microstructure is usually disorganized compared to the alternating copolymers and is more similar to gradient copolymers, which adds additional complexity to their self-assembly/aggregation studies.^{44,45}

Variation in the equimolar ($\pm 5\%$) content of cationic and anionic groups in copolymers was studied due to the importance of a nearly neutral net charge for neglecting disorganized assembly structures.^{31,42,46} Theoretical studies predict that the behavior of a random polyampholyte in aqueous solutions depends on the fraction of ionized repeat units, net charge, added salt, and

polymer chain length.⁴² However, there are few examples in the literature where solutions of poly(cation-*co*-anion) polyampholyte copolymers with non-stoichiometric or predominant content of ionizable groups are prepared, while the ability to form PACs from such copolymers is studied only theoretically.^{43,47,48} This is due to inherent low stability of the polyampholyte solutions, leading to difficulties in preparing their stable solution compositions.^{8,47} Hence, there is a need for further studies of PMAA-based polyampholyte solution stability and self-organization.

Furthermore, earlier, we have developed PMAA nanostructured multilayer hydrogel coatings and microcapsules with polyampholyte-like behavior where the hydrogel volume changes were controlled by ionization of either carboxylic ($\text{pH} > 6$) or amine (at $\text{pH} < 6$) groups with the latter introduced through one-end attached diamine crosslinker of the multilayer coatings.⁴⁹ These polyampholyte-like hydrogels were obtained from polyelectrolyte complexation of PMAA with non-ionic polymers via hydrogen bonding at low pH at template surfaces and have been shown helpful in developing biocompatible responsive multifunctional coatings and particulate materials.^{13,49,50} However, controlled chemical crosslinking of the multilayer coatings of PMAA and a non-ionic polymer has been challenging as a small bifunctional crosslinker was used (*e.g.*, ethylene diamine or adipic acid dihydrazide) and poorly controlled external environmental conditions (*e.g.*, temperature, humidity) could lead to difficulties in consistently controlling the crosslinking degree of the PMAA polyampholyte multilayer hydrogels under the same conditions.

In the present work, we report on the development of poly(methacrylic acid) poly(cation-*co*-anion) statistical polyampholyte copolymers containing primary amine groups (PMAA-NH_2) and excess of carboxylic groups in a polymer chain via subsequent RAFT copolymerization of *tert*-butyl methacrylate and *N*-(*tert*-butoxycarbonyl-aminopropyl)methacrylamide, followed by CTA-end group removal, and cleavage of protected carboxylic and amine groups (deprotection) steps.

The controlled polymerization of monomers and copolymer structures is studied by ^1H NMR spectroscopy, gel permeation chromatography (GPC), and density functional theory (DFT) calculations. The effect of PMAA-NH₂ copolymers with the amine group molar ratios ranging from 3 to 6% on the formation of polyampholyte complexes (PACs) controlled by pH and NaCl concentration was explored by UV-visible spectroscopy and dynamic light scattering (DLS). Previously, most PMAA polymer complexes included a mixture of two oppositely charged homopolymers. Our work is the first example of the formation of PACs from PMAA-NH₂ copolymer with non-stoichiometric content of ionizable groups. The development of PMAA-NH₂ copolymers via controlled copolymerization can lead to facile alternatives for PAC synthesis without using cell-toxic cationic polyelectrolytes such as polyvinylpyridines or polyamines. The copolymers can help develop synthetic routes to novel copolymers and new hydrogel materials with controlled architectures.⁵⁰ This work can also be crucial for understanding the behavior of non-stoichiometric polyampholyte solutions to control polymer chain conformations for further applications of these findings in developing advanced and tunable nanomaterials, including thin nanostructured hydrogels with controlled internal architectures, environmentally adaptable polymeric micro-containers, PAC-based saloplastics, absorbents, anisotropically structured coatings, and biofunctional coatings.

EXPERIMENTAL SECTION

Materials and methods. N-(*tert*-butoxycarbonyl-aminopropyl)methacrylamide (*t*BOC) (98%, uninhibited) was obtained from Polysciences, Inc. and used as received. *Tert*-butyl methacrylate (*t*BMA) (98%, Sigma-Aldrich), 1,4-dioxane (Fisher Scientific), and tetrahydrofuran (THF) (Fisher Scientific) were distilled under reduced pressure and stored under an argon atmosphere. 2,2'-Azobis(2-methylpropionitrile) (AIBN) (98%, Sigma-Aldrich) was recrystallized from methanol

and dried in a vacuum at 20 °C. A chain transfer agent (CTA) 2-cyano-2-propyl benzodithioate (97+%, Aldrich) was used as received. *S*-methyl methanethiosulfonate (97%), *n*-propylamine (99+%), and dichloromethane (99.6%) were from Acros Organics and used as received. Methanol, hydrochloric acid, sodium hydroxide, sodium chloride, and HEPES buffer were from Fisher Scientific (Certified ACS quality) and used as received. Trifluoroacetic acid (TFA) (99.5+%) was used as received from Alfa Aesar. All experiments with aqueous solutions used ultrapure deionized (DI) water with a resistivity of 18.2 MΩ cm.

Synthesis of Poly(methacrylic acid-*co*-(aminopropyl)-methacryl amide) (PMAA-NH₂) copolymers

Copolymerization of *t*BMA and *t*BOC. Poly(methacrylic acid) copolymers with determined content of amine groups, M_w-PMAA-NH₂-*n*, ('*n*' indicates the molar percentage of amine group-containing monomer units in the copolymer, M_w is a rounded weight-average molecular weight in kDa) were synthesized using the reversible addition-fragmentation chain transfer (RAFT) polymerization with subsequent end-group removal and deprotection (Scheme 1). The copolymerization of *t*BMA and *t*BOC was carried out under a nitrogen atmosphere at 65 °C in 1,4-dioxane solution. As an example of a typical copolymerization procedure, the synthesis of 80-PMAA-NH₂-3 is described herein. For that, *t*BOC (0.712 g, 2.94 mmol) was dissolved in 16.8 mL 1,4-dioxane, filtered through a 0.22 μm filter, and injected into the Schlenk tube with a magnetic stirring bar. After that, *t*BMA (5.500 g, 38.68 mmol), AIBN (4.1 mg, 0.0251 mmol), and CTA (12.8 mg, 0.0579 mmol) were added to the reactor. The total amount of 1,4-dioxane was 2.7 mL per gram of monomer, and the ratio of [CTA]/[AIBN] = 2.3 for all studied reactions. After the complete dissolution of components, the mixture was degassed by three freeze-pump-thaw cycles followed by backfilling argon (AirGas) and was heated at 65 °C for 72 h. The reaction was

quenched by immersing the reactor in dry ice. The copolymers were purified twice through precipitation in water/methanol (1:4, v/v) solution and then dried under a vacuum.

Removal of CTA-end group. The end-group modification was carried out through aminolysis in the presence of *S*-methyl methanethiosulfonate. The process started by dissolving 1.0 g of copolymer (pink powder) into 10.0 mL of freshly distilled THF by stirring for 4 hours. Then *S*-methyl methanethiosulfonate and *n*-propylamine were added (the molar ratio of a copolymer, *n*-propylamine, and *S*-methyl methanethiosulfonate was 1:20:40). After 48 hours, the reaction mixture was precipitated in water/methanol (1:2, v/v) mixture followed by drying under a vacuum at room temperature. The resulting copolymer was obtained as a white powder.

Deprotection of carboxylic and amine groups. The copolymer was deprotected by 33% (v/v) TFA in dichloromethane overnight. Typically, 0.60 g of the copolymer from the previous step was mixed with 10.0 mL of dichloromethane and stirred for 4 hours. Then, 5.0 mL of TFA was slowly added to the copolymer solution and stirred overnight at room temperature. The deprotected copolymer was purified by dialysis against DI water using Float-A-Lyzer G2 Dialysis Devices (Repligen; MWCO of 20 kDa) and freeze-dried using a Labconco FreeZone Benchtop Freeze-Drier.

Copolymers characterization. ^1H NMR spectra of the copolymers (15 mg mL $^{-1}$ in CDCl_3 or in D_2O , 99.8 atom% D, Acros) were recorded on a Bruker 400 MHz NMR spectrometer. For some deprotected samples, sodium deuterioxide (NaOD, 40% by mass in D_2O , 99.5% D min, Wilmad) was added to facilitate homogenization. The copolymer molecular mass characterization before group deprotection was performed using Waters chromatographic complex equipped with SDV precolumn guard (PSS, size 8×50 mm, 5- μm particle size) and two SDV 100 000 Å columns (PSS, size 8×300 mm, 5- μm particle size) thermostated at 30 °C. 0.01 M tetrabutyl ammonium

fluoride (TCI) in THF (HPLC grade, Fisher Scientific) was used as an eluent at a 1.0 mL min^{-1} flow rate. GPC traces were recorded on the refractive index detector at $35 \text{ }^{\circ}\text{C}$. The molecular mass and polydispersity of the polymers were calculated using the ReadyCal kit of poly(methylmethacrylate) standards (Agilent).

Turbidimetric analysis. The PMAA-NH₂ copolymers were dissolved in 0.01 M HEPES buffer with or without NaCl (contents varied from 0.1 to 0.3 M) at varied pH values ($2 < \text{pH} < 8$). The absorbance of the copolymer solutions as a function of solution pH was measured using a UV-visible spectrophotometer (Varian-60, Cary Eclipse). The copolymer solution acidity was adjusted by the dropwise addition of HCl or NaOH solutions (0.01 - 3.0 M).

Potentiometric titration. A PMAA homopolymer with $M_w = 45 \text{ kDa}$ (denoted as 45-PMAA) was synthesized via RAFT homopolymerization similar to that for PMAA-NH₂ copolymers. Briefly, *t*BMA (5.0 g, 35.16 mmol), AIBN (7.6 mg, 0.0462 mmol), and CTA (23.5 mg, 0.1065 mmol) were added to the reactor, dissolved in 12.5 mL of 1,4-dioxane followed by freeze-pump-thaw degassing, and polymerized at $65 \text{ }^{\circ}\text{C}$ for 48 h. The obtained polymer underwent the end-group removal step (the molar ratio of a homopolymer, *n*-propylamine, and *S*-methyl methanethiosulfonate was 1:20:40) for 48 hours at room temperature in freshly distilled THF, followed by deprotection in 33% (v/v) TFA in dichloromethane for 24 hours. The deprotected 45-PMAA was purified by dialysis against DI water using Float-A-Lyzer G2 dialysis devices (Repligen; MWCO 20 kDa) and freeze-dried. This 45-PMAA homopolymer was used for pK_a analysis using potentiometric titration. For that, 86.0 mg of 45-PMAA was dissolved in 100 mL of DI water, and a 10.0 mL aliquot of the prepared solution was titrated by 0.01 M NaOH (ACS-certified grade).

Dynamic Light Scattering (DLS). The polymer ζ -potential was monitored by Nano-ZS Zetasizer (Malvern Pananalytical) equipped with He-Ne laser (663 nm) at 25 °C using water as a dispersant and polystyrene latex as a reference material. ζ -Potential average values were acquired with three measurements using the instrument's optimal scanning parameters (ranging from 10-100 scans per measurement) after 5 min equilibration.

Computation. Computations were performed using the Gaussian 16 Revision C.01⁵¹ program on the ASA-X cluster at the Alabama Supercomputer Center, Alabama, USA. The density functional theory (DFT) B3LYP-D3 (Becke three parameters hybrid functional with Lee-Yang-Perdew correlation and empirical Grimme's dispersion)^{52,53} was used for the optimization, single-point energy, and frequency calculations along with the def2-TZVP⁵⁴ basis set. The solvent effects in all steps were evaluated using the conductor-like polarized continuum model (CPCM)⁵⁵ with the default parameters for 1,4-dioxane. Optimized structures were checked to be minima at neutral structures with no imaginary frequencies. The Gibbs free energy for reaction at 65 °C/338 K ($\Delta_r G_{338}$) was computed from the following equations:

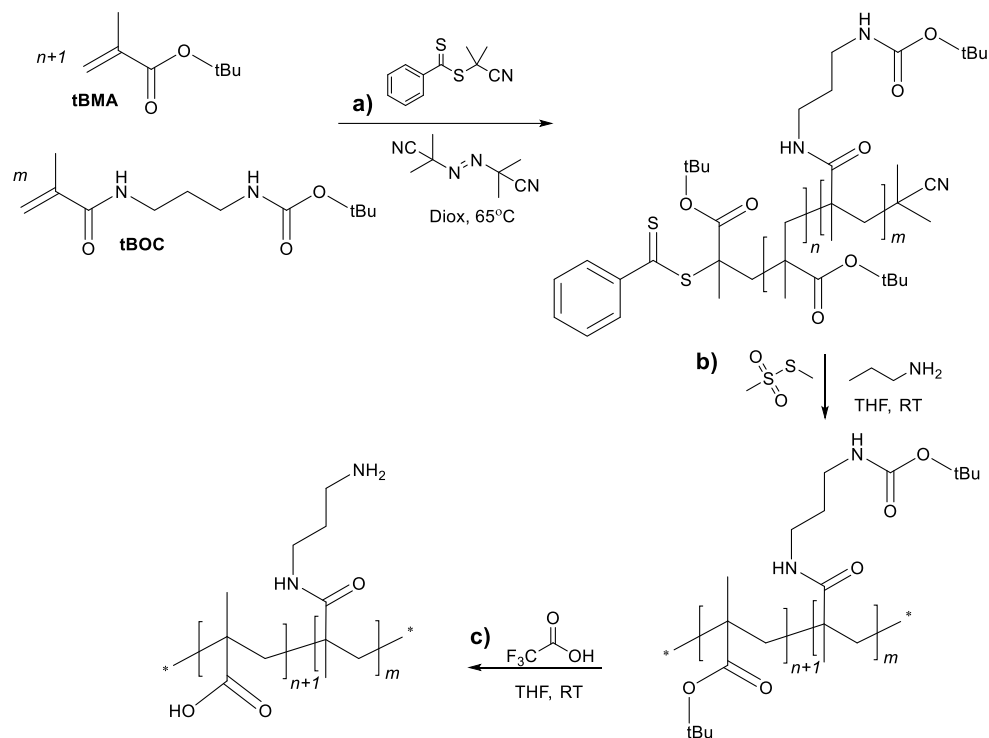
$$\Delta_r G_{338} = \Delta_r H_{338} - T\Delta_r S_{338}$$

$$\Delta_r H_{338} = \Delta E_{\text{total}} + \Delta ZPE + \Delta(H_{338} - H_0)$$

where E_{total} is SCF single point electronic energy, ZPE is the zero-point vibrational energy, $(H_{338} - H_0)$ is the change in enthalpy due to the temperature change from 0 to 338 K, and S is the entropy at 338 K. B3LYP-D3/def2-TZVP level of theory was used due to its recent employment to establish the reaction mechanism and RAFT Equilibrium Constants,⁵⁶ which is a good compromise between quality and efforts.^{56,57}

RESULTS AND DISCUSSION

RAFT polymerization of poly(methacrylic acid-*co*-(aminopropyl)-methacryl amide) copolymers (M_w -PMAA-NH₂-*n*)



Scheme 1. (a) Synthesis of PMAA-NH₂ copolymers via copolymerization of *t*BOC and *t*BMA, followed by (b) CTA end-group removal and (c) deprotection of carboxylic and amine groups.

Copolymerization of unprotected methacrylic acid (MAA) and *N*-(3-aminopropyl)methacrylamide to obtain their uniform copolymers with high molecular weights (> 10 kDa) and low polydispersity can be challenging due to monomer intermolecular interaction and catalyst deactivation in ionic or radical polymerization.^{43,58,59,60,61} Free radical copolymerization^{62,63} of protected monomers was previously reported for synthesis of PMAA-NH₂ copolymers, where control over molecular weight, polydispersity, and microstructure was found challenging. As RAFT polymerization

allows for the molecular weight control by varying monomer to CTA agent ratios,^{43,64} we applied the RAFT-mediated controlled polymerization of *t*BMA and *t*BOC monomers followed by end-group removal and carboxylic and amine group deprotection to obtain PMAA-NH₂ copolymers of controlled molecular weight and structure (**Scheme 1**).

Table 1. Weight-average molecular weight (M_w), Polydispersity (\mathcal{D}), Molar ratio of amine groups (NH₂ mol.%), and the number of NH₂ groups per polymer chain (n) in the PMAA-NH₂ random copolymers synthesized by RAFT.

¹ Sample	² (NH ₂), mol. %	³ M_w , kDa	³ \mathcal{D}	⁴ (NH ₂), mol. %	⁵ M_w , kDa	⁵ \mathcal{D}	⁶ n
45-PMAA-NH ₂ -3	3.0	49.3	1.26	3	48.6	1.30	0.025
45-PMAA-NH ₂ -4	4.8	39.9	1.21	4	41.8	1.26	0.042
45-PMAA-NH ₂ -6	7.5	45.2	1.22	6	44.3	1.23	0.062
80-PMAA-NH ₂ -2	2.5	84.7	1.35	2	83.5	1.36	0.021
80-PMAA-NH ₂ -3	4.2	75.3	1.21	3	74.3	1.22	0.033
80-PMAA-NH ₂ -6	6.9	76.1	1.36	6	81.7	1.34	0.057

¹Sample code = $M_w(\text{theor.})$ -PMAA-NH₂- b , where b is the molar ratio of NH₂-containing units after deprotection. ²Molar ratio of NH₂ group units obtained from ¹H NMR spectroscopy (in CDCl₃) after polymerization step. ³Determined using GPC before deprotection. ⁴Molar ratio of NH₂ group units from ¹H NMR analysis (in D₂O+NaOD) after deprotection. ⁵Determined by GPC after end-group removal. ⁶ n = Number of NH₂ groups per polymer chain/Total number of units per chain.

As reported earlier, (meth)acrylamides (such as *t*BOC) and (meth)acrylates (such as *t*BMA) can be efficiently polymerized via RAFT in the presence of trithiocarbonates and dithiobenzoates.⁶⁵ Herein, 2-cyano-2-propyl benzodithioate was selected as CTA for the copolymerization of *t*BMA and *t*BOC (**Scheme 1a**).^{66,67} We found that RAFT polymerization of *t*BMA to obtain poly(*tert*-

butyl methacrylate) homopolymer in the presence of CTA/AIBN catalytic system in 1,4-dioxane resulted in close to theoretical number-average molecular weights with low polydispersities (**Figure S1**). The *t*BOC homopolymer could not be obtained under these conditions even in a week.

We have previously reported the successful free radical homopolymerization of *t*BOC, where it was used as received without any inhibitors.⁶⁸ Similarly, in this work, the free radical homopolymerization of *t*BOC without 2-cyano-2-propyl benzodithioate (CTA) carried out at $[t\text{BOC}]:[\text{CTA}]:[\text{AIBN}] = 360:0:0.435$ resulted in 65% monomer conversion in 8 hours, unlike 0% conversion in 7 days of *t*BOC polymerization in the presence of the CTA at $[t\text{BOC}]:[\text{CTA}]:[\text{AIBN}] = 360:1:0.435$. We compared the monomer activity in the 2-cyano-2-propyl benzodithioate controlled radical polymerization using DFT calculations using one monomer unit to represent polymer chains (Supporting information, **Figures S2, S3; Table S1**). We found that the intermediate CTA radical with two different monomers on each side of the dithiobenzoate group (**Figure S3, Figure S4a, Table S1**) preferably decomposes to a stable CTA-*t*BOC adduct (**Figure S4b**), releasing active *t*BMA-radical (**Figure S4c**) for cycles of chain propagation. Also, DFT predicts the copolymerization of *t*BOC with *t*BMA due to the small relative energy difference between the formation of CTA-*t*BMA and CTA-*t*BOC adducts. Conversely, this slight difference may lead to a gradient monomer distribution in the final copolymer.⁴⁴

The copolymerization of *t*BMA and *t*BOC monomers was performed at the $[\text{monomer}]/[\text{CTA}]$ ratios of 360 and 720 to obtain the PMAA-NH₂ copolymers with molecular weights of 45 and 80 kg mol⁻¹, respectively (**Table 1**). These molecular weights were chosen to explore the effect of molecular weight on the pH-dependent behavior of PMAA-NH₂ inter/intramolecular PACs. The ¹H NMR analysis of the reaction mixture for the 45-PMAA-NH₂ copolymer synthesis at the

copolymerization time $t = 0$ h (**Figure 1a**) and $t = 72$ h (**Figure 1b**), confirmed the decrease of the monomers' double bond proton signals ($\text{CH}_2=\text{C}(\text{CH}_3)\text{R}$), denoted as a and c in **Figure 1** compared to the integral proton intensity from *tert*-butyl groups ($-\text{C}(\text{CH}_3)_3$), denoted as b .

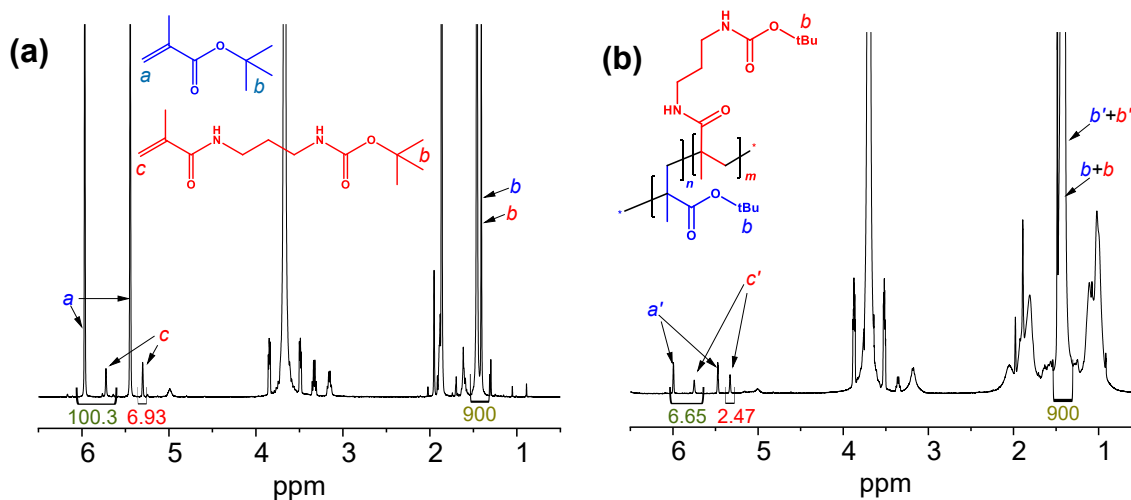


Figure 1. ^1H NMR spectra of initial monomer mixture at the copolymerization time (a) $t = 0$ h and (b) $t = 72$ h after copolymerization to obtain 45-PMAA-NH₂-4 copolymer. In (b), the corresponding monomer signals are marked with a prime symbol.

By comparing the integral intensity of the indicated signals in Figure 1, monomer content and monomer conversion were calculated using the following equations:

$$w_0(\text{tBMA}) = \frac{I(6.0-5.6 \text{ ppm}) - I(5.3 \text{ ppm})}{I(6.0-5.6 \text{ ppm})} \times 100\% \quad (\text{Eq. 1})$$

$$w_0(\text{tBOC}) = \frac{I(5.3 \text{ ppm})}{I(6.0-5.6 \text{ ppm})} \times 100\% \quad (\text{Eq. 2})$$

$$F_{\text{tBOC}} = \frac{I(1.53-1.31 \text{ ppm}) \times 0.01 \times w_0(\text{tBOC}) - 9 \times I(6.0-5.6 \text{ ppm})}{I(1.53-1.31 \text{ ppm}) - 9 \times I(6.0-5.6 \text{ ppm})} \times 100\% \quad (\text{Eq. 3})$$

$$\text{conv}_{\text{total}} = 100\% - \frac{9 \times I(6.0-5.6 \text{ ppm}) \times 100\%}{I(1.53-1.31 \text{ ppm})} \quad (\text{Eq. 4})$$

$$conv_{tBMA} = 100\% \times \left(1 - \frac{9 \times w_t(tBMA)}{w_0(tBMA) \times 0.01 \times I(1.53 - 1.31 \text{ ppm})} \right) \quad (\text{Eq.5})$$

$$conv_{tBOC} = 100\% \times \left(1 - \frac{9 \times w_t(tBOC)}{w_0(tBOC) \times 0.01 \times I(1.53 - 1.31 \text{ ppm})} \right) \quad (\text{Eq.6})$$

where $I(6.0 - 5.6 \text{ ppm})$, $I(5.3 \text{ ppm})$, and $I(1.53 - 1.31 \text{ ppm})$ are the integral intensity of the corresponding region in ^1H NMR spectrum; $w_0(tBMA)$ and $w_0(tBOC)$ are the initial contents of the corresponding monomers, mol.%; $w_t(tBMA)$ and $w_t(tBOC)$ - monomer contents in an unreacted mixture of comonomers, mol.%; F_{tBOC} is the percentage of $tBOC$ monomer units in the copolymer; $conv_{tBMA}$, $conv_{tBOC}$ and $conv_{total}$ correspond to $tBMA$, $tBOC$, and total monomer conversions, respectively.

The experimental M_n was close to the theoretical molecular weight during monomer conversion at the lowest initial $tBOC$ content for 45-PMAA-NH₂-n copolymers with $n = 3, 4$, or 6 (**Figure 2a**). At a higher initial $tBOC$ content, we observed a deviation of the experimental M_n from theoretical values (**Figure 2b and Figure 2c**). Despite that, the dependence of polydispersity, \mathcal{D} , on the conversion resembled the controlled polymerization⁶⁹ and was in the range of 1.10 - 1.30 (**Figure 2b and Figure 2c**). The monomer conversion study revealed that the $tBMA$ monomers were consumed faster than $tBOC$ (**Figure S5**). Also, at about 90% of conversion, the primary polymer chains stopped growing due to a lack of $tBMA$ monomer, high reaction mixture viscosity, and slow monomer diffusion. Additionally, a deviation from the linearity of the first-order plots for both (co)monomers was observed (**Figure S6**). The deviation from linearity shown in Figure S6 is due to the $tBOC$ monomer ability to form more stable radicals with CTA in comparison to $tBMA$. The final increase of $tBOC$ content during the monomer conversion (**Figure S5d**) can be explained by different activities of monomers in copolymerization, which confirmed the predicted $tBOC$ distribution in the final copolymers. A random distribution of monomers is observed when the total conversion is below 80%, where the incorporation fraction of $tBOC$ remains the same

(Figure S5d). The highest effect of gradient monomer distribution was observed for the 45-PMAA-NH₂-6 copolymer with the most amine group units. In this case, the average distance between amine group units in the polymer chain grown at < 80% of the total conversion is three times less than that for the rest of the chain, and the minimum distance between amine groups is eight methacrylic acid units.

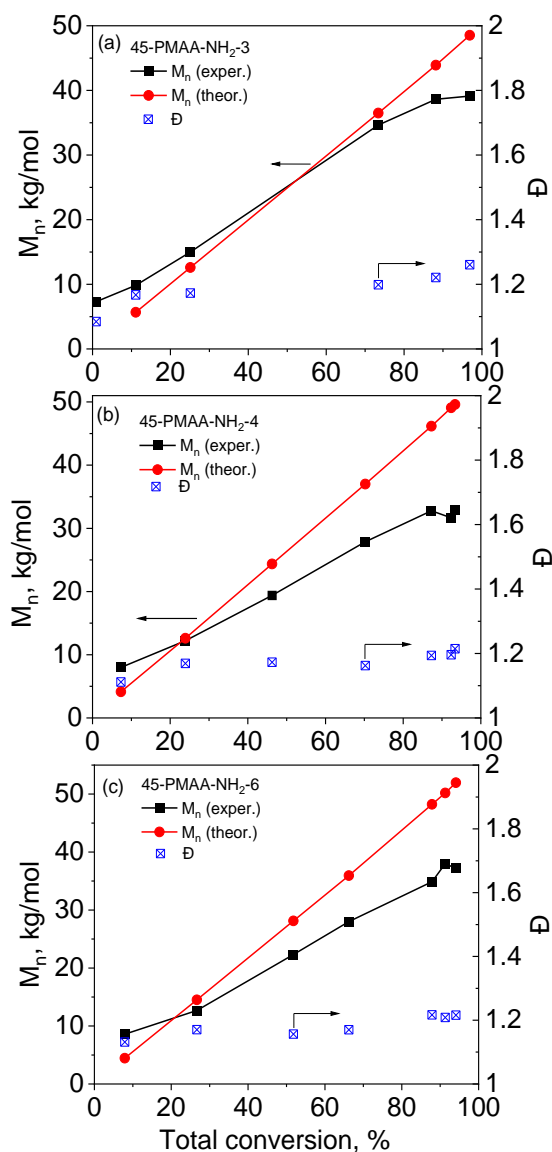


Figure 2. The dependence of number-average molecular weight (M_n), and polydispersity (\bar{D}) on total conversion (%) for the tBMA and tBOC copolymerization for (a) 45-PMAA-NH₂-3, (b) 45-

PMAA-NH₂-4, and (c) 45-PMAA-NH₂-6 copolymers. M_n (theor.) = $\{([tBMA] + [tBOC])/[CTA]\} \times \text{conversion} \times \text{average molecular weight (MW) of monomers} + \text{MW of CTA}$.⁶⁵

After the RAFT copolymerization, the CTA incorporated at the chain end can significantly affect the properties of the final polymer.^{70,71,72} Therefore, the end-groups were removed via aminolysis of the dithiobenzoate end-group (**Scheme 1b**), leading to the disappearance of the pink color due to the dithiobenzoate chain ends (**Figure S7a**). GPC analysis showed similar molecular weight distributions for PMAA-NH₂ copolymers before and after the end-group removal with a slight shift toward the low molecular weights (**Figure S7b**). The molar ratio of NH₂-groups was obtained using ¹H NMR analysis of the PMAA-NH₂ copolymers after hydrolysis of the *tert*-butoxycarbonyl and *tert*-butyl ester protective groups from the integrals of **a** and **b** regions (**Figure 3** and **Figure S8**).

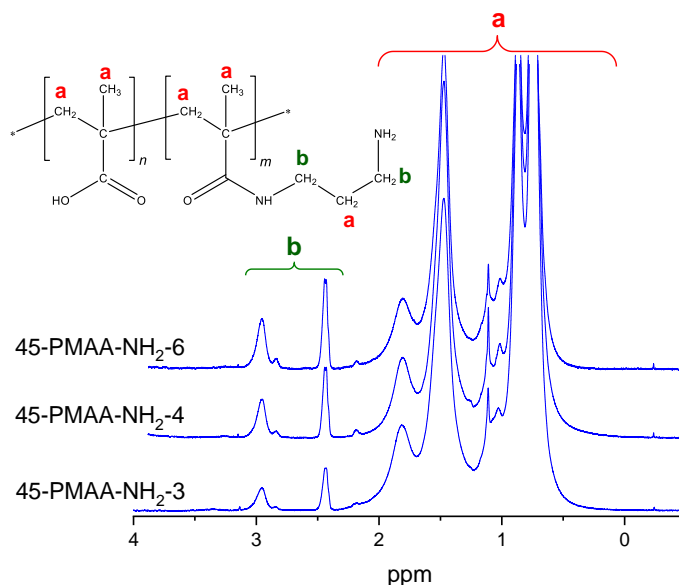


Figure 3. ¹H NMR spectra of 45-PMAA-NH₂ copolymers after hydrolysis of the *t*BOC protective group. Polymer solutions were prepared in D₂O (1.0 mL of 15 mg mL⁻¹ copolymer solution), and a small drop of saturated NaOD (40% by mass in D₂O) was added to the copolymer solution to facilitate its dissolution.

A calculated content of the amine groups tends to decrease after end-group removal and deprotection steps (**Table 1**) due to the decrease in lower molecular weight fractions during copolymer dialysis, that can form at higher monomer conversions and contain more *t*BOC than the main remaining fractions.

pH-Dependent solution behavior of PMAA-NH₂ copolymers: Increasing pH from 2 to 8

The PMAA-NH₂ copolymers obtained in this work are polyampholytes that possess oppositely charged groups on different monomer units and are rich in methacrylic acid content with a low content of primary amine groups. We have shown that this copolymer can be used to produce non-ionic surface assemblies with non-ionic polymers, such as PVPON, at low pH where protonated COOH groups can interact with carbonyls of pyrrolidone lactam rings via hydrogen bonding.^{63,73} However, the formation and stability of PMAA/non-ionic multilayer assemblies formed via hydrogen bonding are dependent on the strength of polymer interaction and, consequently, the degree of PMAA ionization.⁷⁴ For example, PVPON release from the hydrogen-bonded PMAA/PVPON hydrogen-bonded multilayer stable at pH \leq 6.0 could be observed because of a local ionization of the carboxylic groups in the presence of large amounts of positively charged ethylene diamine during the multilayer crosslinking at pH = 5.8.⁶² The disintegration of hydrogen bonds between PVPON and PMAA studied using Fourier transform infrared spectroscopy (FTIR) studies was reported when the PMAA ionization exceeded 15%, while only 5% PMAA ionization could already lead to dissociation of the interpolymer complex between polyethylene oxide (PEO) and PMAA.^{74,75}

Thus, it was crucial to explore the 'polyelectrolyte', *i.e.*, chain extension in deionized water, and 'anti-polyelectrolyte', *i.e.*, chain expansion upon the addition of low molecular weight electrolyte, regimes for the PMAA-NH₂ polyampholyte copolymers to understand their suitability for different

applications (*e.g.*, hydrogen bonding- vs ionic pairing-based copolymer complexes). Herein, we studied the pH-responsive behavior of PMAA-NH₂ copolymers with controlled molecular weights from 45 to 80 kDa, low polydispersity ($\bar{D} < 1.36$), and the controlled ratio of amine-containing monomer units (2-6 mol.%) prepared using our RAFT synthesis.

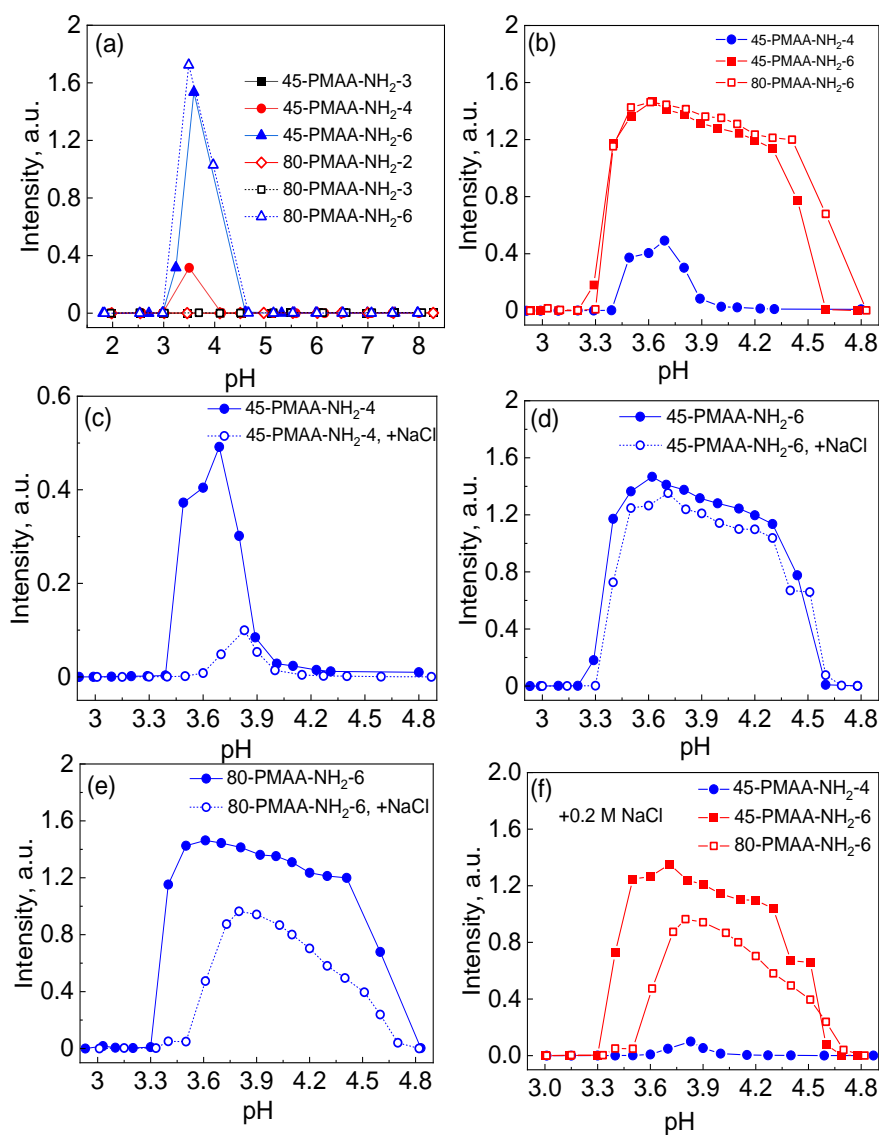


Figure 4. pH-Dependent absorbance of 0.5 mg mL⁻¹ PMAA-NH₂ solutions (0.01 M HEPES buffer) (a, b) without and (c-f) in the presence of 0.2 M NaCl. The acidity of the solutions was increased from pH = 2 to pH = 7. The equilibration time was 55 min for each point.

The potentiometric titration of PMAA homopolymer obtained via RAFT polymerization of *t*BMA followed by end-group and *t*BOC removal (**Scheme 1**) gave pK_a (45-PMAA) = 5.8 ± 0.1 (**Figure S9**), which agrees with previously reported pK_a values of 5.8-6.2 for PMAA. The presence of primary amine groups with pK_b ~ 9.5-10⁷⁶ in PMAA-NH₂ copolymers can lead to inter- and intra-molecular ionic pairing between anionic -COO⁻ and cationic -NH₃⁺ groups in the PMAA-NH₂ copolymers in the pH range from 3.8 to 7.5 where both groups are completely ionized (2 pH units away from pK_a).^{22,33,77} In addition, the formation of interpolymer complexes from water-soluble oppositely charged polyelectrolytes in aqueous solution can depend on the molecular charge, chain length, electrostatic interaction, and ionic strength of the solution.^{42,45,63,77}

Turbidimetric analysis of 0.5 mg mL⁻¹ PMAA-NH₂ solutions (0.01 M HEPES buffer) revealed that PMAA-NH₂-*n* copolymers with the amine group content (*n*) of less than 4 mol.% can behave as polyelectrolytes in the full studied pH range 2 < pH < 8 due to a small net charge at low pH and inherent hydrophilicity of PMAA. Conversely, PMAA-NH₂-*n* copolymers with *n* > 4 mol.% could form aggregates due to the formation of PACs when the solution pH was increased from pH = 2 to pH = 8 (**Figure 4a, Table 1**). Thus, among the six studied PMAA-NH₂ copolymers, only three could produce insoluble PACs, including 45-PMAA-NH₂-4, 45-PMAA-NH₂-6, and 80-PMAA-NH₂-6 with the corresponding ratios of the number of NH₂ groups per polymer chain to the total number of monomer units per chain, *n* = 0.042, *n* = 0.062, and *n* = 0.057 (**Table 1**). Increasing the NH₂ mol.% in the PMAA-NH₂ copolymer from 4 to 6 mol.% resulted in increased scattering from

forming PACs, broadening the pH range where the PACs exist (**Figure 4b**). For example, while the solution turbidity and, thus, PAC could be observed in the range $3.3 < \text{pH} < 4.1$ for 45-PMAA-NH₂-4 (**Figure 4b**, blue spheres), this range broadened for 45-PMAA-NH₂-6 copolymer exhibiting the solution turbidity in the range $3.3 < \text{pH} < 4.6$ (**Figure 4b**, red squares).

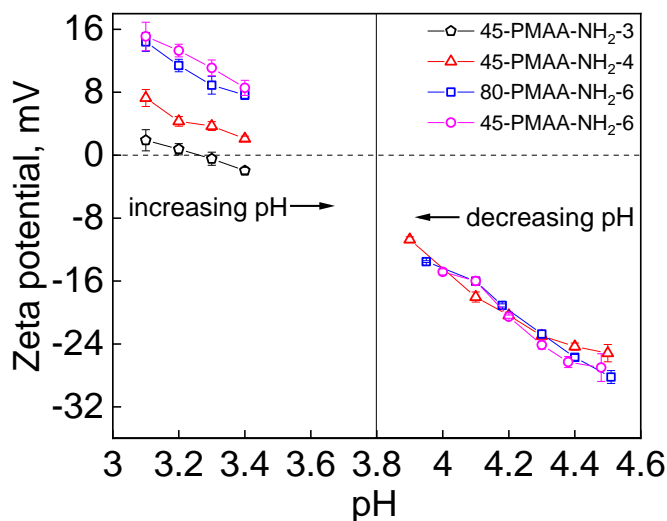


Figure 5. The dependence of the ζ -potential on the PMAA-NH₂ copolymer solution pH. The solution acidity was adjusted from pH = 2 to pH = 7 (left panel) or from pH = 7 to pH = 2 (right panel).

With increasing molecular weight but keeping the same molar ratio of amine groups, the PAC formation from 80-PMAA-NH₂-6 followed a similar trend as for 45-PMAA-NH₂-6 with the same starting pH for PAC formation (pH = 3.3) and slightly extending the range of PAC existence to pH = 4.8 (**Figure 4b**, open red squares). This result correlates well with the fact that 45-PMAA-NH₂-6 and 80-PMAA-NH₂-6 have similar amine group molar ratios. Figure 5 demonstrates that PMAA-NH₂ copolymer solutions exhibit positive ζ -potential values at acidic pH < 3.4 due to

cationic protonated amine groups on the copolymer chains.⁷⁸ Both 45-PMAA-NH₂-6 and 80-PMAA-NH₂-6 had similar ζ -potential values of 15.1 ± 1.8 mV and 14.4 ± 1.2 mV, respectively, at pH = 3.1, which agrees well with the similar NH₂ mole ratios in these copolymers. Similarly, decreasing the amine group mole ratio from 6% to 4% for 45-PMAA-NH₂-4 and to 3% for 45-PMAA-NH₂-3, resulted in the decreased ζ -potential values at pH = 3.1 to 7.3 ± 1.1 mV and 1.9 ± 1.3 mV, respectively (**Figure 5, left panel**).

When the solution pH is gradually raised from pH = 3.1 to 3.4, the ζ -potential values are consistently decreased for all analyzed PMAA-NH₂ copolymers (**Figure 5, left panel**). Although the carboxylic groups are protonated at pH < 3.8 (pK_a = 5.8), the positively charged ammonium groups may, however, induce ionization of protonated carboxylic groups, increasing their ionization value at lower pH compared to that of PMAA homopolymer leading to the onset of PAC formation at a slightly lower pH (**Figure 4**).⁷⁹

We also studied the effect of ionic strength on the pH at which copolymer phase separation occurs and the extent of the pH range where the PAC exists. In all cases, the presence of 0.2 M NaCl in the copolymer solutions resulted in the shift of the PAC formation pH to slightly higher pH values (~0.1-0.2 pH unit higher) compared to the copolymer solution without NaCl, *i.e.*, with lower ionic strength (**Figures 4c-e**). This result indicates that in the presence of 0.2 M sodium chloride, the induced ionization is partially screened due to partial screening of protonated ammonium groups^{8,79,80} and the onset of PAC occurs at a slightly higher pH value due to enhanced solubility of the polyampholyte, so-called 'anti-polyelectrolyte effect' previously reported for polyampholytes.^{81,82} The decreased intensities of the PAC formed in the presence of salt can also indicate a smaller polymer complex size than that without salt due to the increased solubility of copolymer chains^{81,82} (**Figure 4c-e**). Therefore, by summarizing the pH-dependent solution

behavior of PMAA-NH₂ copolymers in the presence of 0.2 M NaCl, we demonstrated that the pH value for the PAC onset could be distinctively shifted from pH ~ 3.3 to ~3.5, and ~3.6 by (1) varying molecular weight of PMAA-NH₂, (2) varying NH₂ mol.%, and (3) adding NaCl to the polyampholyte solution for the copolymers prepared at low pH (≤ 3). In addition, despite some appearance of the gradient amine group distribution in the polymer chain, synthesized PMAA-NH₂ statistical copolymers followed the random formation of water-insoluble polyampholyte complexes differently from alternating copolymers or block-copolymers.^{37,64}

pH-Dependent solution behavior of PMAA-NH₂ copolymers: Decreasing pH from 8 to 2

The copolymer solution turbidity measurements at varied solution pH when the acidity was decreasing from pH = 8 to pH = 2 was measured for 0.5 mg/mL 45-PMAA-NH₂-4, 45-PMAA-NH₂-6, and 80-PMAA-NH₂-6 solutions in 0.01 M HEPES buffer. Unlike the turbidity measurements from low- to high pH, where the 45-PMAA-NH₂-6 and 80-PMAA-NH₂-6 copolymer solutions were turbid up to pH = 4.5 and pH = 4.8, respectively, all the studied copolymer solutions remained clear down to pH = 4.3 (80-PMAA-NH₂-6) (**Figure 6a**).

The 45-PMAA-NH₂ copolymers were slightly more stable regarding the onset of PAC formation, which could be observed at a slightly lower pH of ~ 4.1 (**Figure 6a-c**). The ζ -potential of these copolymer solutions was found to be similar, around -24 mV for all three PMAA-NH₂ studied copolymers at $4.0 < \text{pH} < 4.5$, indicating a high negative net charge of the polyampholytes and their corresponding 'polyelectrolyte regime' behavior.⁸² Therefore, in the pH range from pH = 7.0 to pH = 4.2, unbalanced anionic charge from ionized carboxylic groups led to chain swelling, corresponding copolymer solubility, and solution transparency (**Figure 6a-d**). This behavior was further confirmed by the copolymer solution turbidity analysis in the presence of 0.2 M NaCl. In

all three cases, the addition of salt resulted in the Debye screening of the anionic carboxylates and an earlier formation of PACs at pH = 4.2 (vs. pH = 4.1 at no salt) for 45-PMAA-NH₂-4 (**Figure 6b**), at pH = 4.4 (vs. pH = 4.1 at no salt) for 45-PMAA-NH₂-6 (**Figure 6c**), and at pH = 4.6 (vs. pH = 4.3 at no salt) for 80-PMAA-NH₂-6 (**Figure 6d**). This earlier onset of PAC formation showed a ~0.1 pH unit shift toward higher pH for the copolymer with the lower NH₂ mol.% (n = 4), while that of ~0.3 pH unit shift for the copolymers with the higher NH₂ mol.% (n = 6) regardless of the copolymer molecular weight. Therefore, in the presence of 0.2 M NaCl, the onset of the PAC regime can be well separated for PMAA-NH₂ copolymers initially dissolved at high pH, which can be helpful for the complexation of these polyampholytes with other cationic polyelectrolytes if necessary. In the case of the complexation of these copolymers at surfaces via non-ionic interactions, *e.g.*, hydrogen bonding, the polyelectrolyte regime at 3.9 < pH < 4.2 can be used without salt addition to control multilayer coating thickness.⁸³ The thinner multilayer coatings can be expected then.

A further increase in salt concentration can either lead to additional screening of carboxylates on the chain backbone, subsequent chain collapse and precipitation from solution²⁹ even at pH below or above the onset of PAC formation or disruption of intermolecular interactions between protonated ammonium groups and ionized carboxylic groups in the pH range of PAC existence leading to chain expansion and PAC dissolution (critical salt concentration).^{17,84} Figure 6f demonstrates that increasing NaCl concentration in 45-PMAA-NH₂-6 copolymer solutions from 0.2 M to 0.3 M decreased the solution stability even further with the corresponding onset of PAC formation (turbidity appearance) shift from pH ~ 4.4 (0.2 M NaCl) to pH ~ 4.6 (0.3 M NaCl).

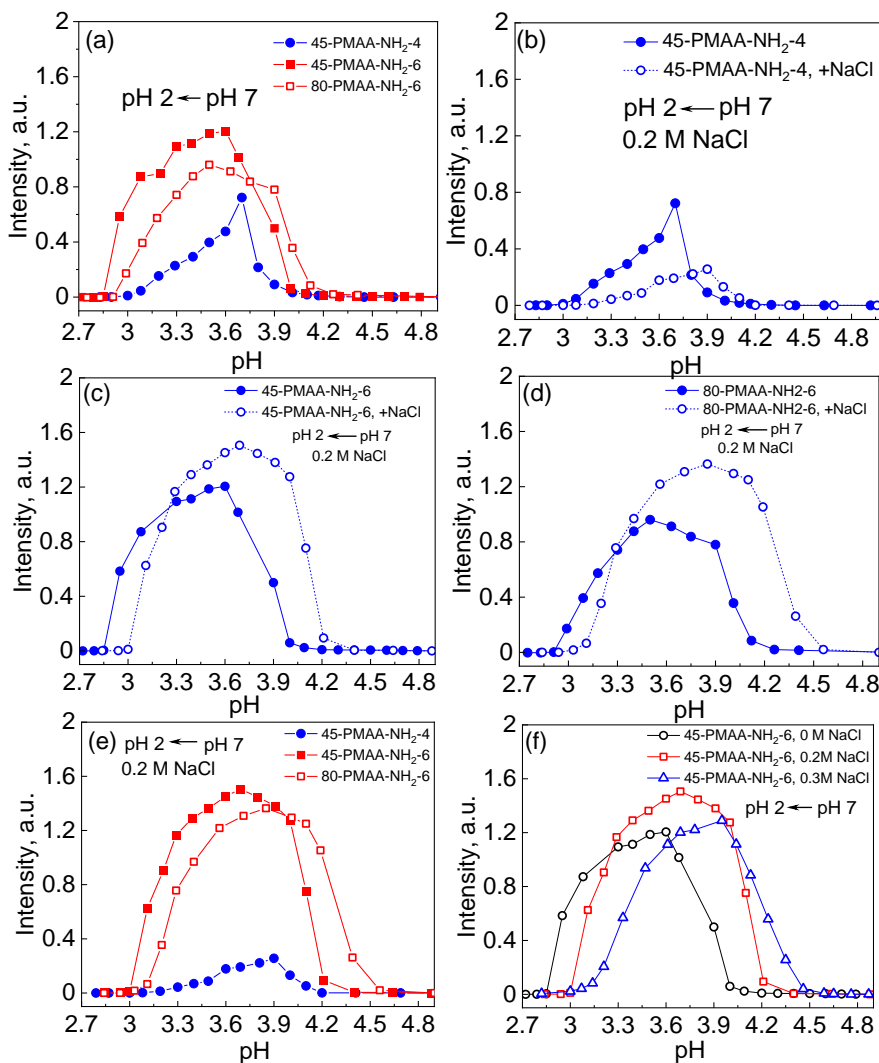


Figure 6. Turbidity of 0.5 mg/mL PMAA-NH₂ solutions (0.01 M HEPES buffer) (a) without salt, or (b-d) with 0.2 M NaCl, measured as the solution absorbance at 400 nm. The initial solution pH was pH = 7 with titration followed from pH 7 to pH 2. An equilibration time was 55 min for each point. (f) Turbidity of 0.5 mg/mL 45-PMAA-NH₂-6 solutions in 0.01 M HEPES buffer in varied amounts of NaCl, measured as the solution absorbance at 400 nm. The solution pH was decreased from pH 7 to pH 2 with an average equilibration time of 55 min for each point.

The results obtained in this work demonstrate that the behavior of COOH-rich PMAA-NH₂ copolymer solutions is similar to the interpolymer interaction between strongly interacting weak polyelectrolytes. Similarly, PMAA-NH₂ copolymers can form large intermolecular aggregates of tens of micrometers in size that are comprised of smaller nanocomplexes, approximately 1 μm in diameter (**Figure S10**) where charge compensation is present and ionic pairs are formed.^{85,86} The pH region where stable PAC can occur for PMAA-NH₂ is relatively narrow (from 3.2 to 4.8) compared to that for PMAA complexes with cationic polyelectrolytes (typically in the 5.0 to 9.0 pH range),⁸⁶ which is determined by the predominant content of COOH groups in the copolymer chain. As a result, polymer chain behavior (polyelectrolyte *vs.* anti-polyelectrolyte) in solution for such poly(cation-*co*-anion) polyampholyte can be tuned by varying the content of amine groups, pH, and salt concentration. Our study showed that the complexing behavior of PACs made from PMAA-NH₂ copolymers is completely reversible. The precise region of PAC formation depends on the initial macromolecular charge balance, defined by a solution pH value. Therefore, a formed water-insoluble PAC can be quickly, on the scale of seconds, turned into water-soluble molecular chains by either decreasing or increasing solution pH beyond the range of PAC existence. These properties can be helpful for the development of advanced biomaterials such as thin film hydrogels, hydrogel-like microcapsules, and internally nanostructured coatings with finely tuned morphology, pH-induced swelling, hydration, and mechanical behavior.

CONCLUSIONS

In this study, we synthesized well-defined poly(*tert*-butylmethacrylate-*co*-N-(*tert*-butoxycarbonyl-aminopropyl)methacryl amide) copolymers (M_w of ~45 kDa and 80 kDa, PDI < 1.36) with different content of amine group (from 2 to 6 mol.%) via subsequent RAFT

copolymerization, end-group removal and carboxylic and amine group deprotection. NMR analysis revealed significant differences in *t*BOC and *t*BMA activities in RAFT copolymerization, which could potentially lead to the gradient monomer distribution in the polymer chain. Despite the absence of *t*BOC homopolymerization, DFT calculations confirmed its copolymerization with *t*BMA and predicted potential gradient copolymerization. The effect of the gradient character of amine group distribution can be diminished when the reaction is quenched at < 80% of total monomer conversion. Also, the minimum distance between amine groups across obtained samples is eight methacrylic acid units, revealing the predominant random character of monomer distribution. The resulting PMAA-NH₂ polyampholyte copolymers can be considered random copolymers due to their low mole fraction of the second monomer in the polymer chain and overestimations of amine group content at the polymerization step. The copolymers with a content of amine groups of more than 4 mol.% can form PACs in a solution in a pH range from 3.2 to 4.8 due to charge compensation and the predominant content of the carboxylic groups. The presence of salt partially screened the ionization of polyampholytes, leading to the onset of PAC formation at a slightly higher pH due to increased solubility, known as the 'anti-polyelectrolyte effect.' Adding NaCl resulted in smaller PAC sizes due to enhanced copolymer chain solubility. The pH for PAC onset could be shifted from ~3.3 to ~3.6 (or from ~4.8 to ~4.1) by varying the molecular weight of PMAA-NH₂, the NH₂ mol.%, adding NaCl, and choosing an initial pH for copolymer dissolution. Despite the potential gradient distribution of amine groups within the non-stoichiometric polyampholyte chain, the synthesized PMAA-NH₂ statistical copolymers formed random, water-insoluble polyampholyte complexes. The PMAA-NH₂ copolymers obtained via controlled copolymerization can lead to facile alternatives for PAC synthesis without using cell-toxic cationic polyelectrolytes such as polyvinylpyridines or polyamines. The gradient

composition of PMAA-NH₂ copolymers obtained at the conversions higher than 80% could be useful in the development of nanostructured coatings with anisotropic charge properties where non-homogeneous charge distribution within surface coating may result in a different pH behavior leading to anisotropic swelling responses. The copolymers can help develop synthetic routes to polyampholytes with controlled architectures useful for synthesizing advanced hydrogel materials with controlled nanostructured architectures, environmentally adaptable microcontinents, PAC-based saloplastics, absorbents, and biomedical coatings.

Author Contributions

P.N. and V.K. equally contributed to this work. P.N. – Investigation, Formal Analysis, Writing and Review/Editing. V.K. - Conceptualization, Data curation, Formal Analysis, Writing and Review/Editing. E.K. - Funding acquisition, Conceptualization, Project administration, Supervision, Validation, Writing - review & editing.

Conflicts of interest

There are no conflicts to declare.

Acknowledgments

This work was funded by NSF CHE award #2419386, partly supported by a grant of high-performance computing resources and technical support from the Alabama Supercomputer Authority. This material is partly based upon work supported under the IR/D Program by the National Science Foundation (E.K.). Any opinions, findings, conclusions, or recommendations

expressed in this material are those of the author(s) and do not necessarily reflect the views of the National Science Foundation.

Footnote[‡]

Electronic supplementary information (ESI) available: The description of DFT calculations, kinetics of homopolymerization, additional ¹H NMR spectra, GPC curves, turbidity, and DLS data are provided.

References

- (1) M. Poudyal, K. Patel, L. Gadhe, A. S. Sawner, P. Kadu, D. Datta, S. Mukherjee, S. Ray, A. Navalkar, S. Maiti, D. Chatterjee, J. Devi, R. Bera, N. Gahlot, J. Joseph, R. Padinhateeri and S. K. Maji, *Nat. Commun.*, 2023, **14**, 6199.
- (2) M. Hoque, M. Alam, S. Wang, J. U. Zaman, Md. S. Rahman, M. Johir, L. Tian, J.-G. Choi, M. B. Ahmed and M.-H. Yoon, *Mater. Sci. Eng. R: Rep.*, 2023, **156**, 100758.
- (3) M. Fu, S.K. Filippov, A.C. Williams, V.V Khutoryanskiy, *J. Colloid Interface Sci.*, 2024, **659**, 849.
- (4) H.G. Abernathy, J. Saha, L K. Kemp, P. Wadhwani, T.D. Clemons, S. E. Morgan , V. Rangachari, *Soft Matter*, 2023,**19**, 5150.
- (5) A. Altun, M. Garcia-Ratés, F. Neese and G. Bistoni, *Chem. Sci.*, 2021, **12**, 12785.
- (6) A. S. Michaels, *J. Ind. Eng. Chem.*, 1965, **57**, 32.
- (7) H. T. Oyama and C. W. Frank, *J. Polym. Sci., Part B: Polym. Phys.* 1986, **24**, 1813.

-
- (8) S. A. Sukhishvili, E. Kharlampieva and V. Izumrudov, *Macromolecules*, 2006, **39**, 8873.
- (9) A. Sathyavageswaran, J. Bonesso Sabadini, S.L. Perry, *Acc. Chem. Res.*, 2024, **57**, 386.
- (10) W. M. Aumiller, F. P. Cakmak, B. W. Davis and C. D. Keating, *Langmuir*, 2016, **32**, 10042.
- (11) Y. Shin and C. P. Brangwynne, *Science*, 2017, **357**, eaaf4382.
- (12) K. A. Black, D. Priftis, S. L. Perry, J. Yip, W. Y. Byun and M. Tirrell, *ACS Macro Lett.*, 2014, **3**, 1088.
- (13) V. Kozlovskaya, E. Kharlampieva, M. L. Mansfield and S. A. Sukhishvili, *Chem. Mater.*, 2006, **18**, 328.
- (14) S. Seidel and G. M. Dianat, *Macromol. Mater. Eng.*, 2016, **301**, 371.
- (15) Z. Qu, H. Xu and H. Gu, *ACS Appl. Mater. Interfaces*, 2015, **7**, 14537.
- (16) U. Ali, K. J. Bt. Abd Karim and N. A. Buang, *Polymer Reviews*, 2015, **55**, 678.
- (17) M. Yang, S. L. Sonawane, Z. A. Digby, J. G. Park and J. B. Schlenoff, *Macromolecules*, 2022, **55**, 7594.
- (18) C. H. Porcel and J. B. Schlenoff, *Biomacromolecules*, 2009, **10**, 2968.
- (19) V. A. Izumrudov, H. O. Ortiz, A. B. Zezin and V. A. Kabanov, *Macromol. Chem. Phys.*, 1998, **199**, 1057.
- (20) Q. Zhao, P. Zhang, M. Antonietti and J. Yuan, *J. Am. Chem. Soc.*, 2012, **134**, 11852.
- (21) A. Reisch, P. Tirado, E. Roger, F. Boulmedais, D. Collin, J.-C. Voegel, B. Frisch, P. Schaaf and J. B. Schlenoff, *Adv. Funct. Mater.*, 2013, **23**, 673.

-
- (22) Z. Sui, J. A. Jaber and J. B. Schlenoff, *Macromolecules*, 2006, **39**, 8145.
- (23) S. T. Dubas and J. B. Schlenoff, *Macromolecules*, 1999, **32**, 8153.
- (24) F. Li, M. Schellekens, J. Bont, R. Peters, A. Overbeek, F. A. M. Leermakers and R. Tuinier, *Macromolecules*, 2015, **48**, 1194.
- (25) S. S. Shiratori and M. F. Rubner, *Macromolecules*, 2000, **33**, 4213.
- (26) J. B. Schlenoff and S. T. Dubas, *Macromolecules*, 2001, **34**, 592.
- (27) A. M. Rumyantsev, E. B. Zhulina and O. V. Borisov, *Macromolecules*, 2018, **51**, 3788.
- (28) Z. A. Digby, M. Yang, S. Lteif and J. B. Schlenoff, *Macromolecules*, 2022, **55**, 978.
- (29) J. B. Schlenoff, A. H. Rmaile and C. B. Bucur, *J. Am. Chem. Soc.*, 2008, **130**, 13589.
- (30) J. J. Madinya, L.-W. Chang, S. L. Perry and C. E. Sing, *Mol. Syst. Des. Eng.*, 2020, **5**, 632.
- (31) M. Ferreira, B. Jing, A. Lorenzana and Y. Zhu, *Soft Matter.*, 2020, **16**, 10280.
- (32) A. Zardehi-Tabriz, Y. Ghayebzadeh, A. E. Gerdroodbar, M. Golshan, H. Roghani-Mamaqani and M. Salami-Kalajahi, *Macromol. Mater. Eng.*, 2023, **308**, 2300179.
- (33) Y. Zhu, J.-M. Noy, A. B. Lowe and P. J. Roth, *Polym. Chem.*, 2015, **6**, 5705.
- (34) J. Niskanen, A. J. Peltekoff, J.-R. Bullet, B. H. Lessard and F. M. Winnik, *Macromolecules*, 2021, **54**, 6678.
- (35) E. Kharlampieva, V. A. Izumrudov and S. A. Sukhishvili, *Macromolecules*, 2007, **40**, 3663.
- (36) J. D. Delgado and J. B. Schlenoff, *Macromolecules*, 2017, **50**, 4454.

-
- (37) B. Saha, N. Choudhury, A. Bhadran, K. Bauri and P. De, *Polym. Chem.*, 2019, **10**, 3306.
- (38) Y. Tao, S. Wang, X. Zhang, Z. Wang, Y. Tao and X. Wang, *Biomacromolecules*, 2018, **19**, 936.
- (39) S. Maji, V. V. Jerca and R. Hoogenboom, *Polym. Chem.*, 2020, **11**, 2205.
- (40) K. Nishimori and M. Ouchi, *Chem. Commun.*, 2020, **56**, 3473.
- (41) P. Sar, S. Ghosh, Yu. D. Gordievskaya, K. G. Goswami, E. Yu. Kramarenko and P. De, *Macromolecules*, 2019, **52**, 8346.
- (42) A. Ciferri and S. Kudaibergenov, *Macromol. Rapid Commun.*, 2007, **28**, 1953.
- (43) B. Kaur, L. D'Souza, L. A. Slater, T. H. Mourey, S. Liang, R. H. Colby and W. T. Ford, *Macromolecules*, 2011, **44**, 3810.
- (44) M. Semsarilar and V. Abetz, *Macromol. Chem. Phys.*, 2021, **222**, 2000311.
- (45) S. E. Kudaibergenov and A. Ciferri, *Macromol. Rapid Commun.*, 2007, **28**, 1969.
- (46) L. D. Blackman, P. A. Gunatillake, P. Cassa and K. E. S. Locock, *Chem. Soc. Rev.*, 2019, **48**, 757.
- (47) A. V. Dobrynin, R. H. Colby and M. J. Rubinstein, *Polym. Sci., Part B: Polym. Phys.*, 2004, **42**, 3513.
- (48) W. Zhang, Y. Ma, N. D. Posey, M. J. Lueckheide, V. M. Prabhu and J. F. Douglas, *Macromolecules*, 2022, **55**, 6750.
- (49) V. Kozlovskaya, M. Dolmat and E. Kharlampieva, *Langmuir*, 2022, **38**, 7867.

-
- (50) M. Dolmat, V. Kozlovskaya, J. F. Ankner and E. Kharlampieva, *Macromolecules*, 2023, **56**, 8054.
- (51) Gaussian 16, Revision C.01, M. J. Frisch, G. W. Trucks, H. B. Schlegel, G. E. Scuseria, M. A. Robb, J. R. Cheeseman, G. Scalmani, V. Barone, G. A. Petersson, H. Nakatsuji, X. Li, M. Caricato, A. V. Marenich, J. Bloino, B. G. Janesko, R. Gomperts, B. Mennucci, H. P. Hratchian, J. V. Ortiz, A. F. Izmaylov, J. L. Sonnenberg, D. Williams-Young, F. Ding, F. Lipparini, F. Egidi, J. Goings, B. Peng, A. Petrone, T. Henderson, D. Ranasinghe, V. G. Zakrzewski, J. Gao, N. Rega, G. Zheng, W. Liang, M. Hada, M. Ehara, K. Toyota, R. Fukuda, J. Hasegawa, M. Ishida, T. Nakajima, Y. Honda, O. Kitao, H. Nakai, T. Vreven, K. Throssell, J. A. Montgomery, Jr., J. E. Peralta, F. Ogliaro, M. J. Bearpark, J. J. Heyd, E. N. Brothers, K. N. Kudin, V. N. Staroverov, T. A. Keith, R. Kobayashi, J. Normand, K. Raghavachari, A. P. Rendell, J. C. Burant, S. S. Iyengar, J. Tomasi, M. Cossi, J. M. Millam, M. Klene, C. Adamo, R. Cammi, J. W. Ochterski, R. L. Martin, K. Morokuma, O. Farkas, J. B. Foresman and D. J. Fox, Gaussian, Inc., Wallingford CT, 2019.
- (52) A. D. Becke, *J. Chem. Phys.*, 1993, **98**, 5648.
- (53) S. Grimme, J. Antony, S. Ehrlich and H. Krieg, *J. Chem. Phys.*, 2010, **132**, 154104.
- (54) F. Weigend and R. Ahlrichs, *Phys. Chem. Chem. Phys.*, 2005, **7**, 3297.
- (55) M. T. Cancès, B. Mennucci and J. Tomasi, *J. Chem. Phys.*, 1997, **107**, 3032.
- (56) M. Werner, J. C. A. Oliveira, W. Meiser, M. Buback and R. A. Mata, *Macromol. Theory Simul.*, 2020, **29**, 2000022.
- (57) Ü. Yıldırım, A. Ç. Ata, A. A. Tanrıverdi and I. Çakmak, *Bull Mater Sci*, 2021, **44**, 186.
- (58) M. Ye, D. Zhang, L. Han, J. Tejada and C. Ortiz, *Soft Matter.*, 2006, **2**, 243.

-
- (59) M. Pitsikalis, in *Ionic Polymerization. Reference Module in Chemistry, Molecular Sciences and Chemical Engineering*; Elsevier, 2013.
- (60) M. Fantin, A. A. Isse, A. Venzo, A. Gennaro and K. Matyjaszewski, *J. Am. Chem. Soc.*, 2016, **138**, 7216.
- (61) J. Scheerder and H. Langermans, *Colloid Polym Sci*, 2014, **292**, 991.
- (62) V. Kozlovskaya, J. F. Alexander, Y. Wang, T. Kunczewicz, X. Liu, B. Godin and E. Kharlampieva, *ACS Nano*, 2014, **8**, 5725.
- (63) V. Kozlovskaya, Y. Wang, W. Higgins, J. Chen, Y. Chen and E. Kharlampieva, *Soft Matter*, 2012, **8**, 9828.
- (64) G. Moad, E. Rizzardo and S. H. Thang, *Aust. J. Chem.*, 2009, **62**, 1402.
- (65) S. Perrier, *Macromolecules*, 2017, **50**, 7433.
- (66) M. Benaglia, E. Rizzardo, A. Alberti and M. Guerra, *Macromolecules*, 2005, **38**, 3129.
- (67) P. Yang, L. P. D. Ratcliffe and S. P. Armes, *Macromolecules*, 2013, **46**, 8545.
- (68) V. Kozlovskaya, A. Shamaev and S. A. Sukhishvili, *Soft Matter*, 2008, **4**, 1499.
- (69) B. Yu and A. B. Lowe, *J. Polym. Sci. A Polym. Chem.*, 2009, **47**, 1877.
- (70) H. Willcocka and R. K. O'Reilly, *Polym. Chem.*, 2010, **1**, 149.
- (71) C. P. Jesson, C. M. Pearce, H. Simon, A. Werner, V. J. Cunningham, J. R. Lovett, M. J. Smallridge, N. J. Warren and S. P. Armes, *Macromolecules*, 2017, **50**, 182.

-
- (72) C. H. Hornung, K. Känel, I. Martinez-Botella, M. Espiritu, X. Nguyen, A. Postma, S. Saubern, J. Chiefari and S. H. Thang, *Macromolecules*, 2014, **47**, 8203.
- (73) V. Kozlovskaya, B. Xue, M. Dolmat and E. Kharlampieva, *Macromolecules*, 2021, **54**, 9712.
- (74) S. Sukhishvili and S. Granick, *Macromolecules*, 2002, **35**, 301.
- (75) E. Kharlampieva and S. A. Sukhishvili, *J. Macromol. Sci.C: Polym. Rev.*, 2006, **46**, 377.
- (76) V. S. Bryantsev, M. S. Diallo and W. A. Goddard, *J. Phys. Chem.*, 2007, **111**, 4422.
- (77) J. K. Bediako, J.-H. Kang, Y.-S. Yun and S.-H. Choi, *ACS Appl. Polym. Mater.*, 2022, **4**, 2346.
- (78) V. Kozlovskaya and S. A. Sukhishvili, *Macromolecules*, 2006, **39**, 6191.
- (79) E. Kharlampieva and S. A. Sukhishvili, *Langmuir*, 2003, **19**, 1235.
- (80) V. Izumrudov, E. Kharlampieva and S.A. Sukhishvili, *Macromolecules*, 2004, **37**, 8400.
- (81) A. B. Lowe and C. L. McCormick, *Chem. Rev.*, 2002, **102**, 4177.
- (82) A. V. Dobrynin, R. H. Colby and M. Rubinstein, *J. Polym. Sci. B Polym. Phys.*, 2004, **42**, 3513.
- (83) E. Kharlampieva, V. Kozlovskaya and S. A. Sukhishvili, *Adv. Mater.*, 2009, **21**, 3053.
- (84) M. Tirrell, *ACS Cent. Sci.*, 2018, **4**, 532.
- (85) C. E. R. Edwards, K. L. Lakkis, Y. Luo and M. E. Helgeson, *Soft Matter*, 2023, **19**, 8849.

-
- (86) K. O. Margossian, M. U. Brown, T. Emrick and M. Muthukumar, *Nat. Commun.*, 2022, **13**, 2250.

Data for this article will be available upon request. This manuscript will be available at <https://www.ekharlamgroup.com/>.